1993 CEDAR Workshop
Boulder, Colorado
June 21-26, 1993

CEDAR Prize Lecture

by John Cho
Arecibo Observatory

Radar Scattering from the Coldest Place in Our Atmosphere: Polar Mesosphere

Radar Scattering from the Coldest Place in Our Atmosphere: Polar Mesosphere Summer Echoes

John Y. N. Cho
Arecibo Observatory, Arecibo, Puerto Rico

Preface

First, let me tell you that I'm about to do something I've never done before. That is to read a scientific paper from a prepared text. For some reason, this is hardly ever done and seems to be a taboo. But in other fields it's rather the norm. In many respects, it would seem to be even better suited to a scientific talk, providing for precision of expression and economy of words. Probably fewer AGU talks will go past the inevitable 12-minute time limit, the speaker frantically shuffling through the last 2/3 of his or her viewgraphs as that little traffic light begins to blink red and the convenor nervously stands up to signify stop. Perhaps it's a bad idea to try my experiment on such a large audience, but on the other hand, the eye contact that I'm abandoning will likely make no difference in this big setting–if you're going to fall asleep, you're going to fall asleep regardless of whether I'm glancing in your direction. Some of you have heard me give talks before, so you can tell me afterwards which way you like better. Provided you kept awake throughout.

So let me begin.

Intro

The summer polar mesopause is the coldest region of our atmosphere. (At the end of the talk, I will discuss the possible asymmetry between the arctic and the antarctic, but for now we'll stick to the term "polar.") [Figure 1.] Here we have rocket-launched falling-sphere temperature measurements made by Frank Schmidlin during the noctilucent cloud campaign in Sweden in the summer of '91. Note that the mesopause temperature in one instance is below 100 K. This is the lowest natural temperature measured in our atmosphere. Even average temperatures are thought to be around 120 K in the summer polar mesopause.

Why is the temperature so low? And why is it lower in the summer when the sun is shining continuously than in the dark winter? [Figure 2.] In a nutshell, the global circulation pattern in the mesosphere is one of summer to winter, with upward motion at the summer pole cooling adiabatically and downward flow at the winter pole warming compressionally. (You can see this in the bottom figure.) In effect, the summer mesosphere is being cooled by a global refrigerator which counteracts the heating of the summer sun. The pump for the refrigerator is provided by breaking gravity waves that transfer momentum to the mean flow, spinning it up at the summer pole and spinning it down at the winter pole. Conservation of angular momentum and continuity completes the circulation cell. The sense of flow is determined by the fact that only gravity waves with eastward phase speeds make it up to the mesopause due to the filtering effects of the westward stratospheric flow. And the reverse is true on the winter side.

So, we can already see that the cold mesopause is a classic CEDAR type of problem.

Let me mention that, even though this is a good theory and most people believe it, the only long-term observations of the mean vertical flow in the polar mesosphere seem to contradict it. [Figure 3.] There appears to be a significant *downward* flow in the upper mesosphere in the summer according to this multi-year composite average of the 50-MHz Poker Flat radar data. It turns out that one of the bonuses of our radar scattering theory is that it helps to explain this discrepancy.

As the direct result of the extremely low temperatures, the highest clouds in our atmosphere also form in the summer mesopause. [Figure 4.] These are known as noctilucent clouds (or NLC for short), because they are so tenuous that you can only see them after the sun has dipped below the horizon, turning the sky dark, but still illuminating the mesosphere from below. Of course, this means that there are limited windows of time and latitude in which you can see them, but satellites have been able to observe what are known as polar mesospheric clouds (or PMC) covering the entire polar regions which may, in fact, be the same as NLC.

These clouds have received attention lately as a possible indicator of global change. Since their formation and brightness are sensitive to the temperature and water vapor content, they should serve as a visible sign of change in either parameter. Since increase in atmospheric CO_2 is believed to lower the mesopause temperature, and an increase in methane gas is thought to increase the water content, an increase in both of these greenhouse gases is projected to make for brighter and more frequent clouds. This has, indeed, been observed for over 20 years.

Finally, in the same region that produces the low temperatures and clouds, it was discovered a little over a decade ago that radar waves were scattered extremely strongly–orders of magnitude more than existing theory could account for. [Figure 5.] Here we have the original observations with the 50-MHz Poker Flat radar. The altitude range and the season of their occurrence corresponded very well to the cold summer mesopause. In the bottom plot you can see that the summer signals are much higher than the winter signals. They became known as polar mesosphere summer echoes (or PMSE).

To give you an idea of the physical morphology of PMSE, I can show you this plot made from CUPRI, which is a portable, 50-kW, 50-MHz radar operated by Cornell. [Figure 6.] The top panel shows signal strength versus height and time, the middle shows vertical velocity, and the bottom shows spectral width. Note that PMSE usually occur in thin layers. You can also see a nice example of a gravity wave in the velocity plot. Thus, one of the benefits of PMSE is that even small radars can observe the dynamics of the summer mesopause region.

Main Text

Now, there are various interesting characteristics of PMSE, but the main puzzle was their incredibly high signal strength. This is the question I will be focusing on today: Why are PMSE signals so strong?

The short answer to this question was provided by rockets measuring the electron density structure. [Figure 7.] These plots compare electron density fluctuation spectra from the polar summer mesosphere, the polar winter mesosphere, and the equatorial mesosphere. Note that at the Bragg wavenumber of a 50-MHz radar, there is several orders of magnitude more power in the electron density fluctuation in the polar summer than in the polar winter or in the equatorial region. Since the radar echo strength is dependent on this quantity, it certainly explains why PMSE are so strong.

But then the question becomes: Why is there so much more structuring in the electron density in the summer polar mesosphere?

[Figure 8.] To reiterate the basics for a moment, radar Bragg scatter results from refractive index inhomogeneities which, in the mesosphere, is dominated by electron density inhomogeneities. Their existence depends on a perpetual struggle between the generation mechanisms and diffusive dissipation. So, to increase the radar scatter, either the generation rate must be raised or the electron diffusion must be lowered, or both.

Non-PMSE type echoes in the mesosphere can be explained well by the structuring of electron density by neutral dynamics, usually turbulence. This is, in fact, what one would expect for the generation mechanism, since the electron density is only about one part in 10^{10} of the neutral density. Since there is absolutely no evidence for (or any reason to believe that) turbulence is incredibly intense in the summer mesosphere, other people have suggested different generation mechanisms that invoke special chemical or electrodynamic processes. They could be right, but there's not much evidence to support the existence of these other generation processes. But my point is that, regardless of the generation mechanisms, if we can find a way to lower the electron diffusion, then we can explain the strong PMSE signals.

[Figure 9.] So. We needed to look at electron diffusion in the mesosphere. Because of the electric field coupling, electrons and ions are constrained to diffuse in an interactive manner. This is known as ambipolar diffusion. To illustrate this phenomenon, I have what is called my "Cow and Black Fly" analogy.

First, imagine releasing a boxful of black flies in the middle of an empty field. They disperse very quickly, owing to their high random speeds. These are the electrons. Now imagine herding a bunch of cows to the center of the pasture and releasing the flies with them. The grazing cows diffuse away at much slower random speeds, and the black flies are constrained to follow the cows due to the natural attraction to *their* food supply. The cows are ions and the attraction is the electric force. Thus, we see that electron diffusion is slowed down by the presence of ions.

The first idea that was proposed was that heavier ions might slow the diffusion further. Heavier ions do, in fact, exist in the summer mesopause. Because of the low temperatures, water molecules can cluster around a proton. These hydrated protons can get pretty heavy and they may even act as nucleation sites for further growth into cloud particles. But as it turns out, their diffusivity is only proportional to the inverse square root of the reduced mass, so no matter how heavy the ions became, the diffusion could not be slowed down significantly. This is because the ion-neutral interaction is characterized by polarization interaction.

But then I thought: There are much *larger* particles up there, some even large enough to be visible from the ground as clouds! And we know that these aerosols interact with the neutrals more-or-less as hard spheres. Hard sphere interaction yields a diffusivity dependency which is an inverse square of the radius. So, the larger the particle, the slower its diffusion.

Comparing the interaction cross sections for polarization versus hard sphere models, we estimate that the transition from one to the other takes place for a singly charged particle when its radius is about 5 angstroms. This roughly corresponds to a cluster ion with 20 water molecules. So particles larger than this can start to have dramatically lower diffusivities.

Generally speaking, however, the larger the aerosol, the fewer their number. So there was a question of whether there are enough large particles to make an overall impact on the plasma ambipolar diffusion. So we needed to quantify this process.

[Figure 10.] These are the quasi-neutral diffusion equations for a weakly ionized, three-species plasma, that is, electrons, positive ions, and aerosols of any charge. I'll forgo the mathematical details and simply say that a simple one-dimensional numerical study of these equations yielded the following results.

[Figure 11.] The vertical axis here is the normalized electron diffusivity and the horizontal axis is effectively the measure of how much of the total plasma charge is tied up in the aerosols. The different curves correspond to different aerosol sizes. The top plot is for positively charged aerosols, and the bottom one is for negatively charged aerosols.

Note that, as expected, larger aerosols reduce the diffusivity more, but that this effect doesn't really kick in until the total charge on the aerosols exceed somewhat more than half of the total plasma charge of the same sign. This is the transition you see here. Note also that both positively and negatively charged aerosols are effective in reducing the diffusivity. For reasons to be explained later, we need a reduction in electron diffusivity by about two orders of magnitude to explain the signal strengths of PMSE, so from this plot we see that we need aerosols with radius on the order of 0.01 microns. This is well below the average size of visible cloud particles and are probably sub-visible ice particles themselves.

To satisfy the charge criterion, we need either a large amount of charge on a small number of particles, or a small amount of charge on a large number of particles. To examine this question we need to turn to model calculations, since there is extremely little observational data on the number, size, and charge states of summer mesopause aerosols.

First, if we assume that the aerosols are purely ice, then the equilibrium of electron and ion current to the aerosol yields a slightly negative charge of -1 to about -4 for the largest, that is visible, particles. This pretty much rules out highly multiply charged aerosols, and we would need a few thousand per cubic centimeter of these aerosols with a charge of -1 or -2 to account for PMSE signal strengths. NLC simulations by Turco et al. show that a few thousand per cc of 0.01 micron ice particles are reasonable.

[Figure 12.] So we have here a mini-summary of the most likely state of charged aerosols that effectively enhances radar scatter in the summer mesopause. As a bonus, these parameters also happen to agree pretty well with George Reid's calculation of the kind of aerosols which might be causing the electron density bite-outs often observed in the region of PMSE. [Figure 13.] Here are two rocket electron density measurements superimposed on the radar signal profiles. Note the large density depletion in the right-hand plot co-located with the PMSE layer. The idea is that these ice particles are scavenging the ambient electrons to create a depletion layer. [Figure 12.] We can also say that, because these particles responsible for PMSE are substantially smaller than the visible NLC particles, PMSE should exist at a somewhat higher altitude than NLCs. This is statistically true: the peak average occurrence of PMSE is at 86 km, whereas the average NLC height is around 83 km. [Figure 14.] And the first simultaneous measurement of PMSE and NLC that we made during the NLC-91 campaign showed likewise that PMSE was at a higher height than NLC.

Now, previously I said that a two-order magnitude reduction in electron diffusivity was required to explain PMSE echo strengths. I will take a moment to justify that statement. [Figure 15.]

If we believe that neutral turbulent advection is a generation mechanism for electron density fluctuations in the summer mesosphere (and there is increasing evidence that it is at least one of the major generation mechanisms), then we can quantify the effect of decreased diffusivity (or equivalently, an increased Schmidt number, where the Schmidt number is the ratio of the neutral viscosity to the electron diffusivity). Normally in the upper mesosphere, the Schmidt number is about one and the viscous cut-off and the diffusive cut-off occur at about the same scales. As the Schmidt number is increased, however, the diffusive cut-off extends further to smaller and smaller scales. [Figure 16.] This is a model calculation of radar reflectivity for very intense turbulence in the mesopause region. The two curves correspond to Schmidt numbers 1 and 100. The vertical bars are the range of PMSE reflectivities observed at three different radar frequencies. Note the tremendous leverage that the Schmidt number (or equivalently diffusion reduction) has in enhancing the echo power at radar Bragg scales normally beyond the viscous cut-off. It appears that a Schmidt number of 100 (and hence, the two-order magnitude reduction in electron diffusivity) does quite well at explaining even the strongest PMSEs at VHF.

Note, however, that PMSE at 933 MHz (and also 1290 MHz, not shown here) are more problematic. According to our reduced diffusion theory, they would require even larger aerosols, which, due to their smaller numbers would have to be highly multiply charged. Some have argued that this is possible if the ice aerosols are contaminated by metallic elements from meteoric dust which lower their photoelectric work function such that they can become highly positively charged by sunlight. If such a "dusty plasma" scenario is considered, a totally different radar scattering enhancement can take place, which I call "dressed aerosol scatter."

[Figure 17.] A multiply charged aerosol in a plasma will acquire a "Debye sphere" of a net surplus or debit of electrons around it, depending on the sign of the aerosol charge. If the radar wavelength is substantially longer than the associated dusty plasma Debye length, then the electron density perturbation will respond in phase. If you go through the calculations, it turns out that the radar scattering enhancement over the incoherent scatter level is linearly proportional to the aerosol charge. There is a further restriction that these "Debye spheres" not overlap with each other, so in effect, the aerosols have to be fairly highly charged and relatively far apart. So, dressed aerosol scatter as candidate for explaining PMSE at ultra high frequencies is a possibility but problematic.

However, there is one other piece of data that prefers the scenario of large, highly charged aerosols. [Figure 18.] Recall that there is a discrepancy between the theoretical upward flow in the summer mesosphere of about 1 cm/s versus the radar-observed downward average velocity of about 30 cm/s. This apparent downward velocity would correspond to the fall speed of a 0.07 micron ice sphere. The radar would only respond to the inhomogeneities in electron density following what might be called the snow fall, and would not see the upward motion of the vaporized water and the mean flow.

Before I make a brief summary statement, I would like to give you a news update from Antarctica. The first search for PMSE in the southern polar mesosphere by Ben Balsley et al. yielded no trace of them. In retrospect, this may not be such a surprising discovery, as there is evidence pointing to a warmer mesopause over the Antarctic. First, there is less gravity wave activity in the south, which logically leads to an observed weaker meridional circulation. Satellite measurement of polar mesospheric clouds also show that arctic clouds are inherently brighter than antarctic clouds. All of this points to a warmer mesopause and fewer aerosols. The few temperature measurements that exist do point to a warmer mesopause in the south. It could very well be that the lack of orography in the southern hemisphere–it's mostly ocean, after all–to force gravity waves is resulting in a warmer mesopause. This sounds to me like a great CEDAR-type project for someone to work on.

Summary

[Figure 19.] In summary: Charged aerosols can dramatically enhance radar scatter in the mesosphere. And their presence also helps to explain electron density "bite-outs" and the radar-observed mean downward flow in the summer mesosphere.

In light of the non-observation in the south, we may have to rename this phenomenon to yet another stupid acronym, different and yet the same: Summer Arctic Mesopause Echoes.

T ≤ 100 K

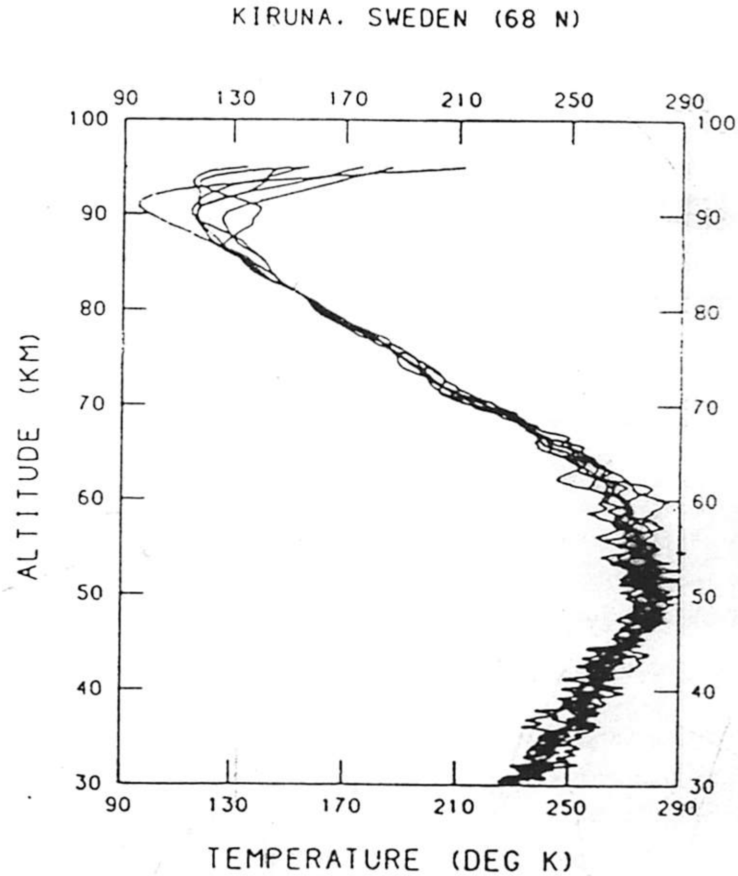

Schmidlin - 1992

#1

Fig. 1

Why is the summer mesopause so cold?

(1) Without gravity wave forcing

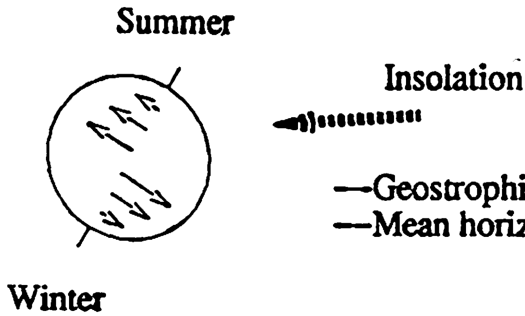

—Geostrophic winds are set up
—Mean horizontal flow increases with height

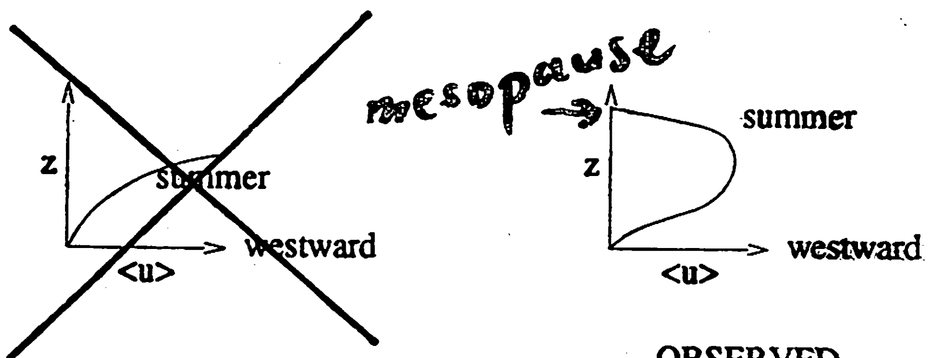

NOT OBSERVED!

OBSERVED.

(2) With gravity wave forcing

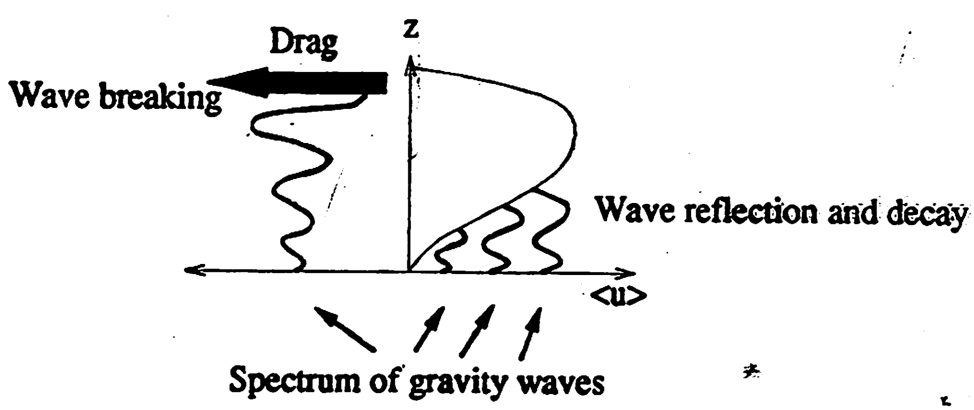

Meridional circulation

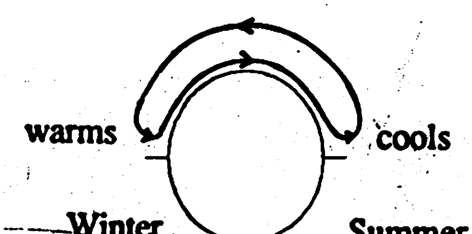

Fig. 2

VERTICAL VELOCITY

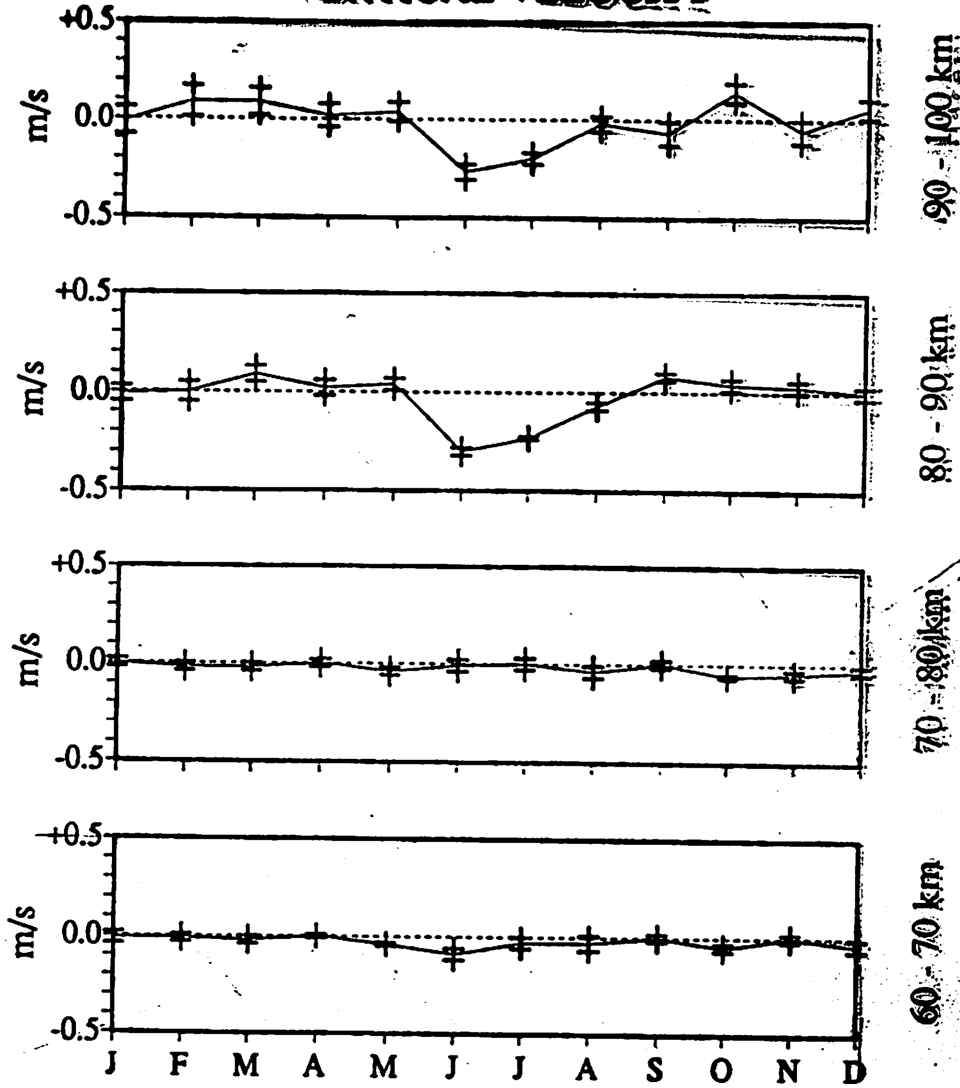

Composite year of monthly mean vertical velocities formed from the years 1979 - 1983 inclusive, and the height bins between 60 and 100 km. Positive is upward. Notice that the velocity scale is changed by a factor of 100 from that on the horizontal velocity plots. The upper two height bins show a *downward* summer flow of 20 to 30 cm/s. The magnitude and sign of this motion is in direct contradiction to the circulation theory. In fact, the meridional and vertical velocity measurements taken together appear to violate mass continuity.

[Hall et al., 1992]

Fig. 3

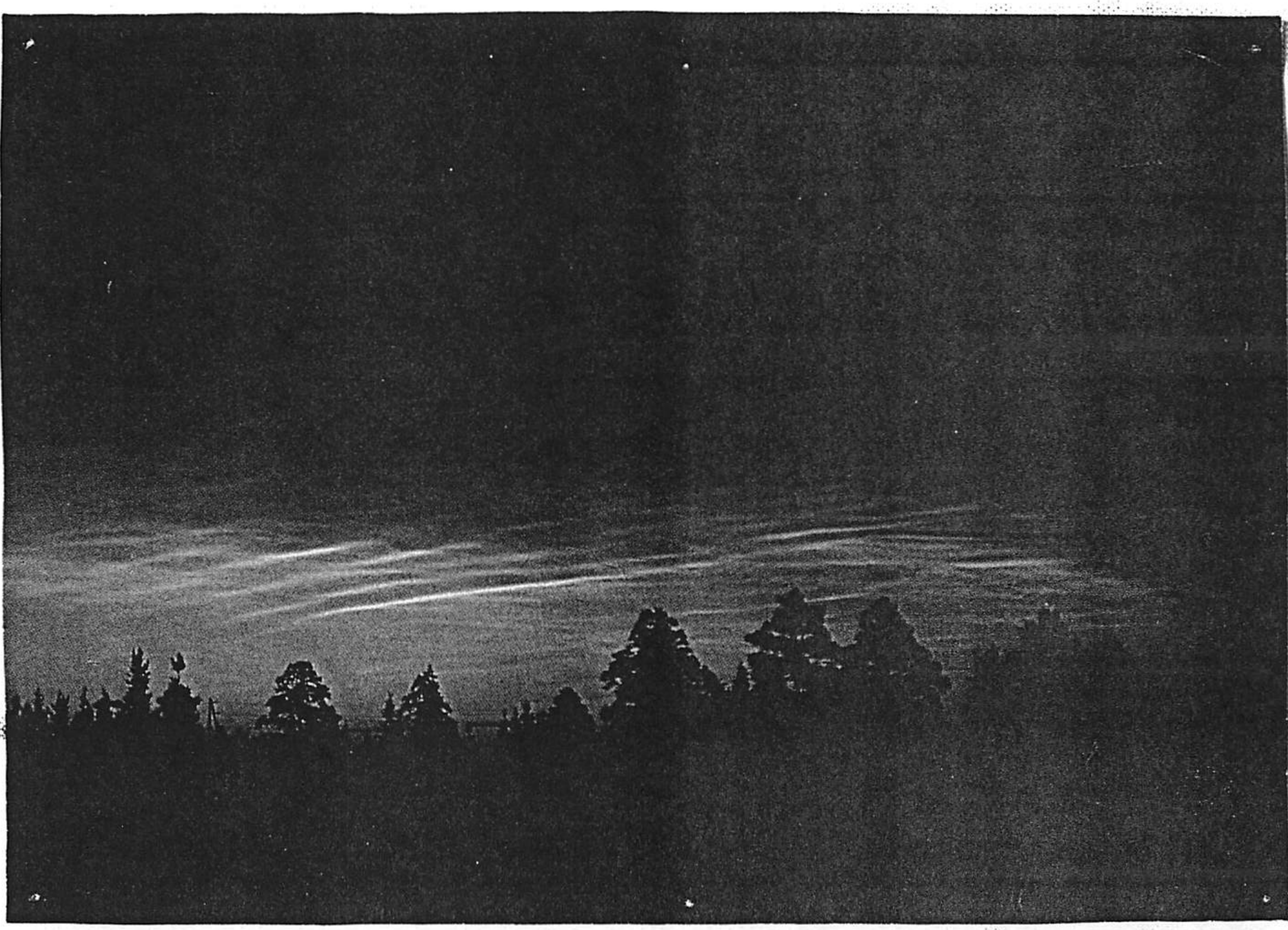

Fig. 4

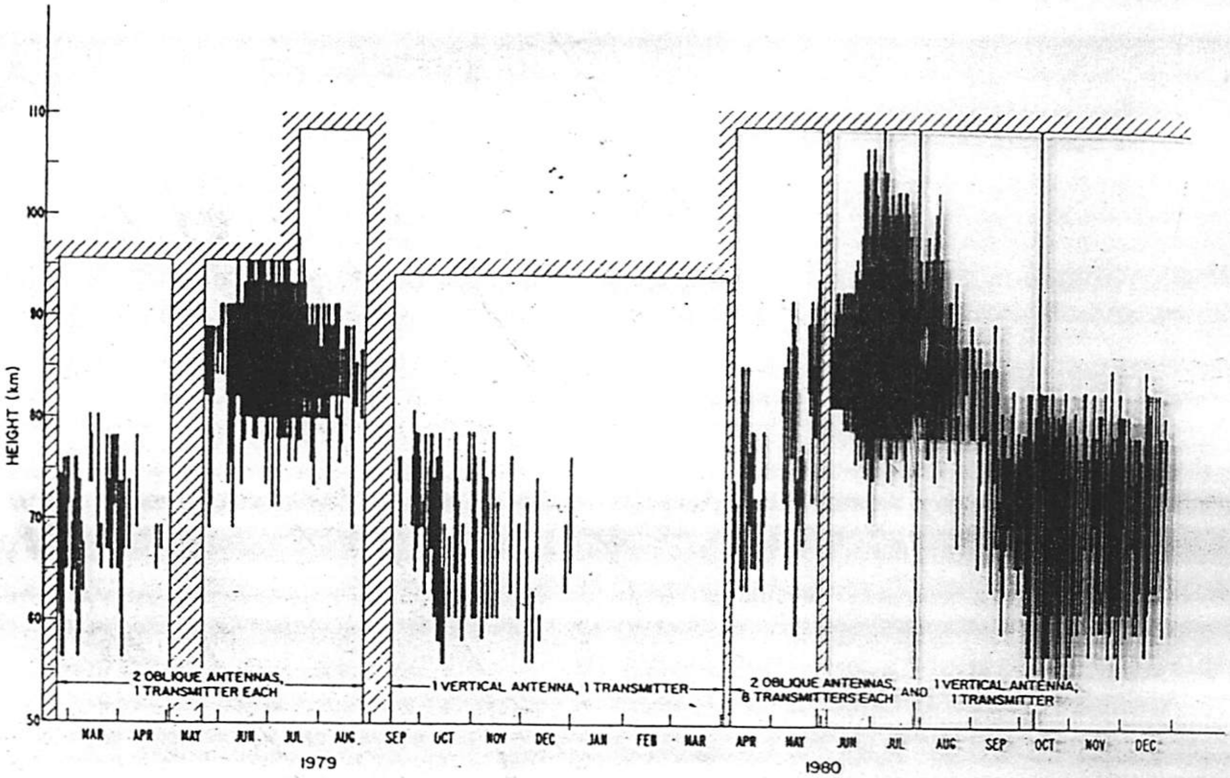

FIG. 1. The height distribution of echoes as a function of time of year (from Ecklund and Balsley, 1981). Hatched areas indicate times or height ranges of no data. Note the relatively sharp transition between the summer and winter echo height distributions.

enhanced signal levels of the Poker Flat summer echoes relative to the midlatitude echoes suggest a separate generating mechanism. In addition, Ecklund and Balsley (1981) noted the close correspondence between the 86 km height of the summer echo maximum and the strong temperature minimum at the summertime mesopause.

On the basis of their existing evidence, Ecklund and Balsley (1981) concluded that the mesospheric echoes arose from intense neutral turbulence operating on a vertical electron density gradient. The turbulence was suggested to arise from a non-local source (e.g., the breakdown of upward-propagating, tropospherically-generated gravity waves). Gravity wave breakup at mesospheric heights has been proposed by many workers (e.g., Hines, 1960; Hodges, 1967; Lindzen, 1981; Weinstock, 1976, 1982; Dunkerton, 1982a). Specifically, Lindzen (1981) has proposed that the seasonal height dependence of the Poker Flat echoes arises from the fact that, because of seasonal variation of the intervening zonal wind profile, the energy density of the summertime gravity waves is weaker, so that they break up at the higher heights.

In this paper, we present additional results of our continuing investigation of the mesospheric echo generation mechanisms. Our current ideas of the causal mechanisms for the winter echoes are in line with our earlier ideas; the mechanism for the summer echoes,

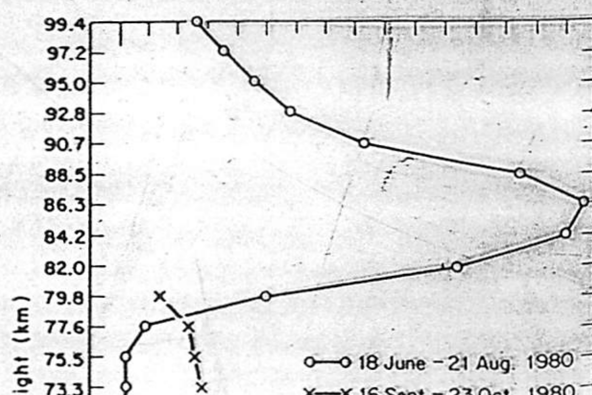

FIG. 2. Time-averaged height profile of signal-to-noise ratio for typical summer (18 June–21 August 1980 curve) and winter (16 September–23 October 1980 curve) conditions (from Ecklund and Balsley, 1981).

Fig. 5

18

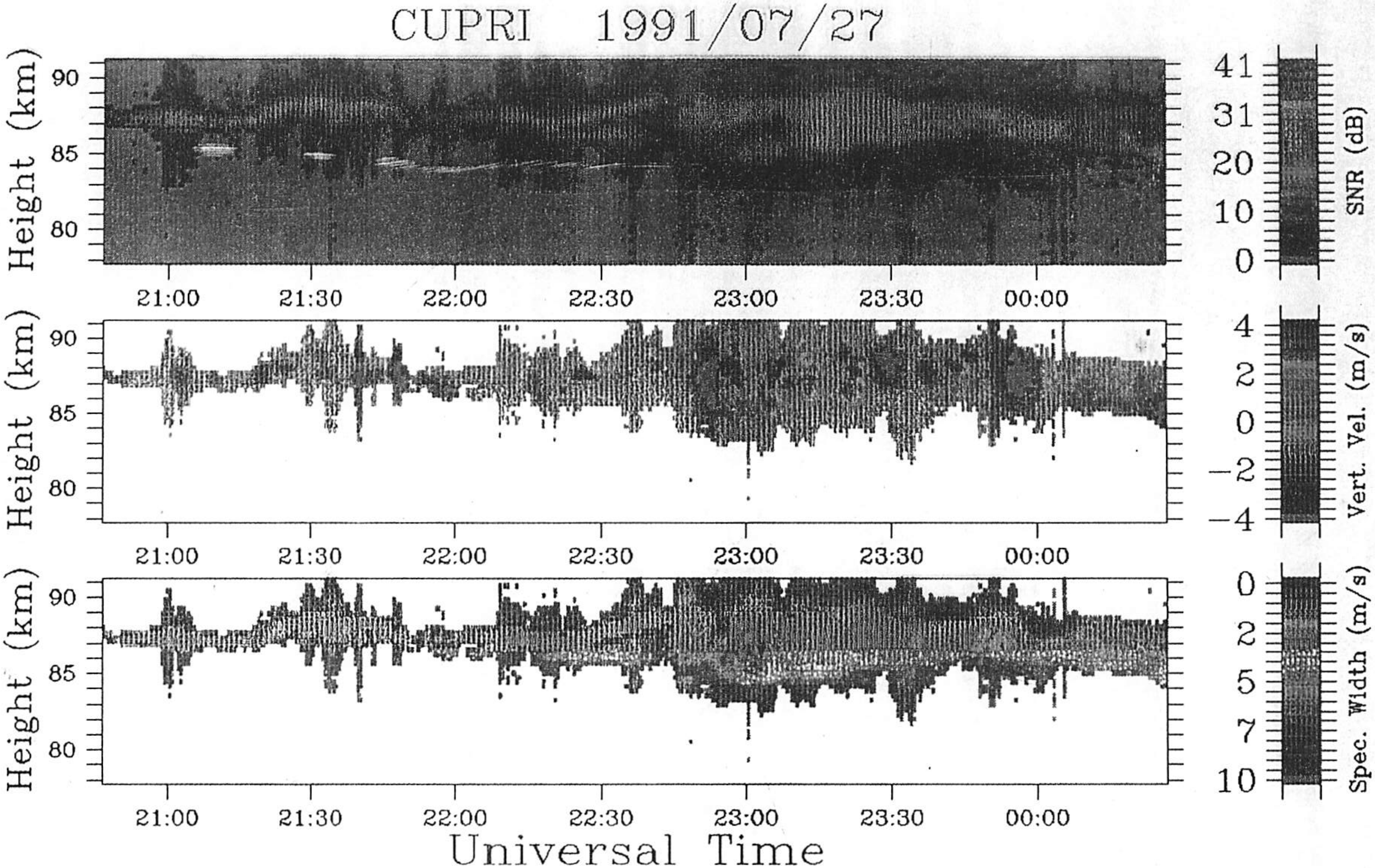
CUPRI 1991/07/27
Height (km)
90
85
80
21:00
21:30
22:00
22:30
23:00
23:30
00:00
41
31
20
10
0
SNR (dB)
4
2
0
−2
−4
Vert. Vel. (m/s)
0
2
5
7
10
Spec. Width (m/s)
Universal Time

Fig. 6

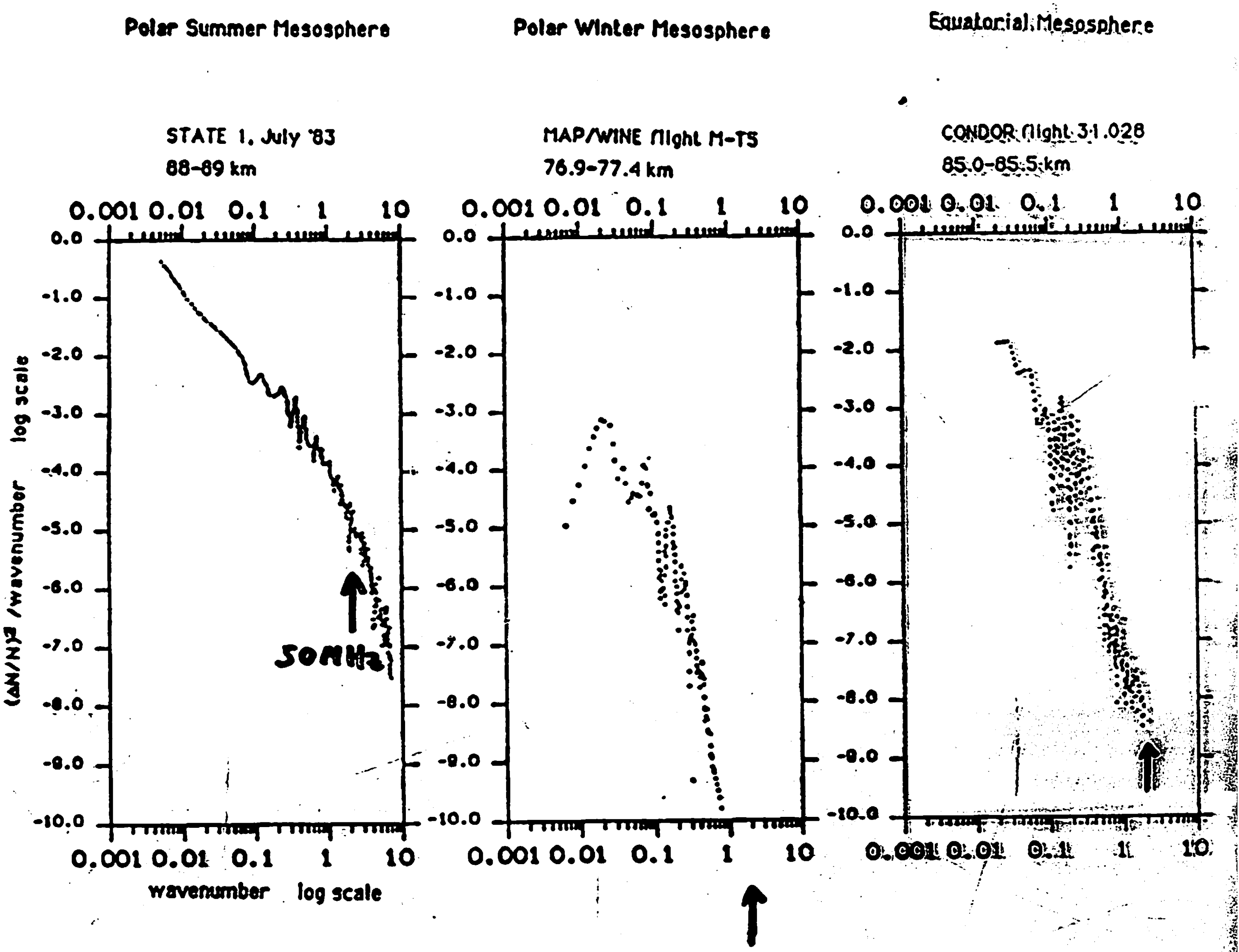

Comparison of mesospheric electron density data from polar summer, polar winter, and equatorial rocket launches [*Ecklund et al.*, 1988; *Blix*, 1988; *Røyrvik and Smith*, 1984].

Fig. 7

The Basics of Mesospheric Coherent Radar Scatter

Radar scatter

↑

Refractive index inhomogeneities

↑

Electron density inhomogeneities

<u>Generation</u>

Neutral dynamics
  Turbulence
  Stratification
  Gravity waves

Non-PMSE

Chemistry
  Localized recombination

Photochemistry
  Localized ionization

Electrodynamics
  Plasma waves
  Electric fields

<u>Dissipation</u>

* Electron diffusion

PMSE?

Either generation ↑
and/or dissipation ↓

Fig. 8

Electron Diffusion in the Mesosphere

- Ambipolar diffusion: cow & fly analogy
- What can dramatically lower D_e?
  - $H^+(H_2O)_n$? [Kelley et al, 1987]

$\Rightarrow$ NO. Polarization interaction

$\longrightarrow D \propto \mu_{in}^{-1/2}$ $\quad \mu_{in} = \frac{m_i m_n}{m_i + m_n}$

- Charged aerosols?

$\Rightarrow$ Possible! Hard sphere interaction

$\longrightarrow D \propto \mu_{an}^{-1/2} r_a^{-2}$

- Transition size

$$D \propto \begin{cases} \mu_{an}^{-1/2} & r < r_{crit} \\ \mu_{an}^{-1/2} r_a^{-2} & r > r_{crit} \end{cases}$$

$r_{crit} \simeq 5 Å \rightarrow H^+(H_2O)_{20}$

Fig. 9

Model: Quasi-neutral diffusion of weakly ionized 3-species plasma

Generalizing equations of *Hill* [1978] to multiple charges:

$$\frac{\partial n_c}{\partial t} = \frac{|Z_a|D_+ + Z_+D_a}{Z_+ + |Z_a|}\nabla^2 n_c + \left[\frac{D_+ - D_a}{Z_+ + |Z_a|} + \left(1 - \frac{N_a}{N_e}Z_a\right)D_+ - \frac{N_a}{N_e}|Z_a|D_a\right]\nabla^2 n_e$$

$$\frac{\partial n_e}{\partial t} = \frac{|Z_a|D_+ - Z_+D_a}{Z_+ + |Z_a|}\nabla^2 n_c + \left[\frac{D_+ + D_a}{Z_+ + |Z_a|} + \left(1 - \frac{N_a}{N_e}Z_a\right)D_+ + \frac{N_a}{N_e}|Z_a|D_a\right]\nabla^2 n_e$$

$$n_c = n_+ \pm n_a$$

Numerical simulation:

- Introduce sinusoidal perturbation to densities (proportional to background density ratios).
- Measure e-folding time T for electron density perturbation.
- Calculate effective electron diffusion coefficient

$$D_e \equiv 1/k^2$$

Fig. 10

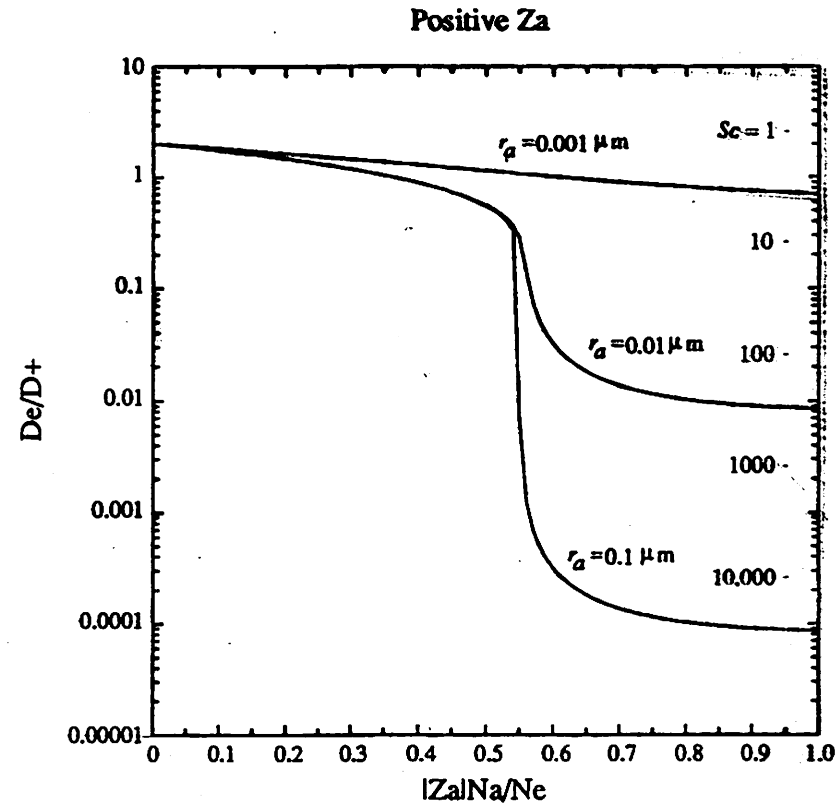
Positive Za
De/D+
|Za|Na/Ne
r_a=0.001 μm
r_a=0.01 μm
r_a=0.1 μm
Sc= 1
10
100
1000
10,000

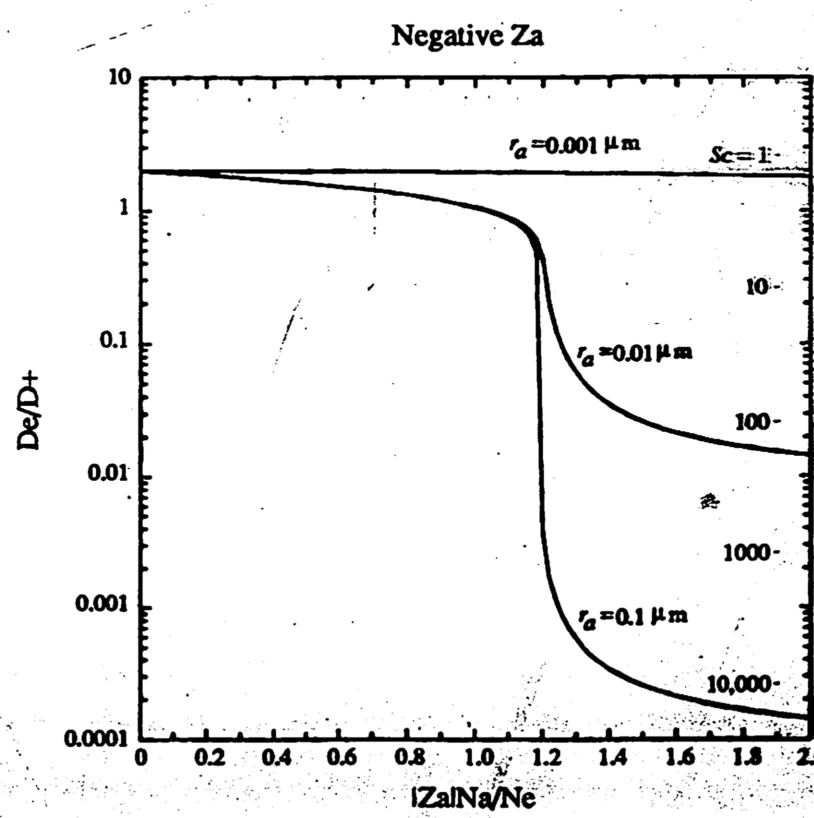
Negative Za
De/D+
|Za|Na/Ne
r_a=0.001 μm
r_a=0.01 μm
r_a=0.1 μm
Sc= 1
10
100
1000
10,000

Fig. 11

Some Conclusions

- The radar cross sections of VHF PMSE can be explained by charged ice aerosols with

$\rightarrow$ $r_a \sim 0.01\,\mu m$

$z_a \sim -1, -2$

$N_a \sim$ few thousand cm^{-3}

i.e., a large number of small low negative charge ice particles.

- This also agrees with Reid [1990]'s calculation of electron density bite-outs:

$r_a \sim 0.01\,\mu m$

$z_a \sim -1$

$N_a \sim 1000\,cm^{-3}$

- Prediction: VHF PMSE occur higher than NLC.

(statistically true. PMSE @ 86 km
NLC @ 83 km)

Fig. 12

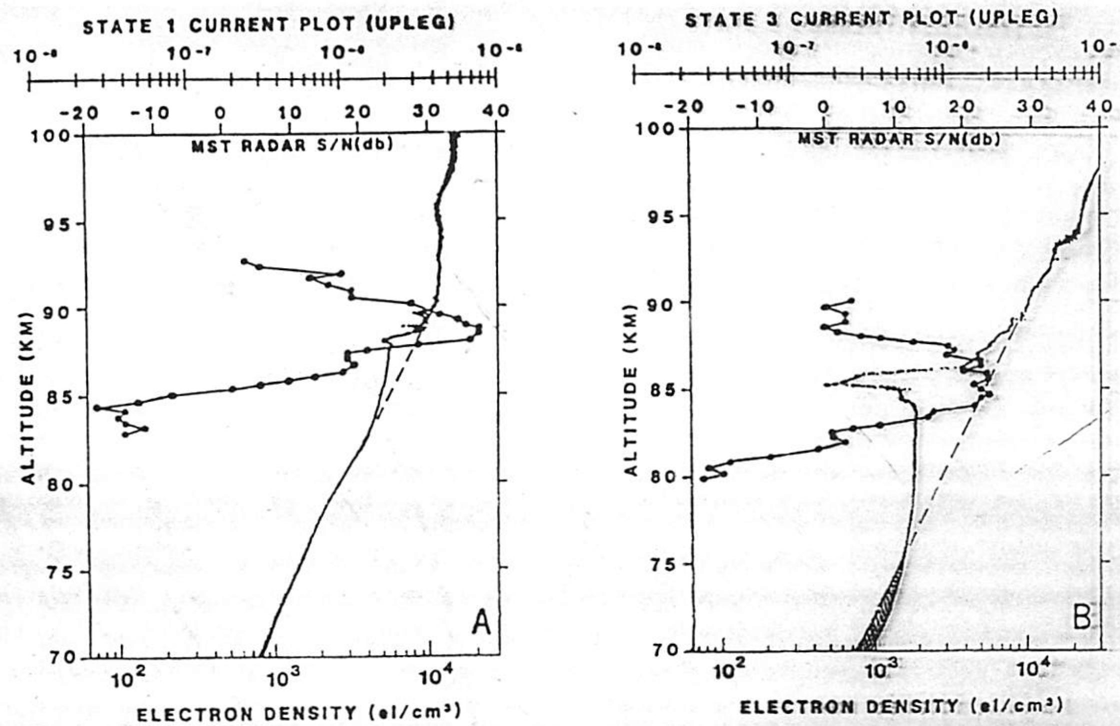

Fig. 3. Height profiles of the rocketborne dc probe results and MST radar echo S/N (solid circles) for the (*a*) STATE 1 and (*b*) STATE 3 rocket flights. The dc probe results are given both in (top scale) probe current and (bottom scale) tentative electron density values, assuming a constant proportionality between the two (see text). The dashed lines illustrate a more typical *D* region profile.

gions of most intense radar backscatter. It should be noted that the STATE 1 S/N peak in the radar data is about 37 dB near 88 km, whereas the STATE 3 S/N is much weaker and lower, reaching a peak of only 23 dB near 85 km. The STATE 3 results suggest that the region of radar backscatter corresponds to the altitude of steep gradients in the electron density caused by a deep "bite-out" in the electron density of almost an order of magnitude at 86 km. For STATE 1, however, the rapidly changing structure in the electron density and the corresponding sharp rise in the radar return power occur above the small depletion (about 10%) in the electron density profile near 88 km. Note that both electron density profiles are not typical of the normal *D* region. The STATE 3 profile is particularly atypical in that the vertical electron density gradient is almost zero from 77 to 84 km. (The dashed lines in Figures 3*a* and 3*b* emphasize this).

A power spectral analysis of the probe data was performed following the method of *Blackman and Tukey* [1958]. Spatial power spectra of the relative electron density fluctuations were first calculated from 2048 data points, corresponding to a time series of about 0.25 s to a height resolution better than 150 m in the altitudes of prime interest. This time series allowed the data to be spectrally analyzed in a frequency range extending to over 4000 Hz (i.e., a spatial resolution corresponding to scale sizes of about 12 cm). This resolution is considerably finer than the 3-m structure to which the 50-MHz radar is sensitive. In addition, longer time series were analyzed, using 2048 data points over 0.5-, 1.0-, 2.0-, 4.0-, and 8.0-s intervals, to examine the spectra at the lower frequencies (longer scale sizes). During these measurements the rocket spin rate was near 22 revolutions s^{-1}. Under these conditions, even tip-mounted probes suffer from some contamination at the spin frequency which is visible in the power spectra, if the data are treated as is usually done by constructing deviations from a running mean. Since the spin effects were so prominent in the data, an attempt was made to remove these as much as possible by detrending the data, using a 12-term polynomial fit to the data. Power spectral analysis was conducted on both rocket data sets, and these will be discussed individually in the following paragraphs and then compared both with the radar data and with each other.

Fig. 13

2.2. *STATE 1*

Inspection of the STATE 1 electron density results and the radar data in Figure 3 suggests that the power spectral analysis should be done in two time/altitude intervals: (1) from 95 to 111 s (76–85.8 km), where there were no strong radar echoes, and (2) from 111 to 123 s (85.5–92 km), where there were significant radar echoes.

2.2.1. *Interval from 95–111 s (76–85.8 km).* These data were spectrally analyzed in two time intervals, as shown in Figure 4*a*. No turbulent structure is apparent in the electron current measurements shown in interval 1, which is dominated by rocket spin effects. The power spectrum of these data shown in Figure 4*b*, shows the only significant spectral component to be at the spin frequency (approximately 22 Hz). Interval 2 of Figure 4*a* exhibits more structure in the current data, and the corresponding spectrum in Figure 4*c* shows a distinct increase in fluctuation power at frequencies below 10 Hz. It should be noted in Figure 4*c* that the noise level at high frequencies decreased with increasing altitude compared with Figure 4*b*, an effect which was also observed by *Royrvik and Smith* [1984] in their investigation of mesospheric turbulence in Peru.

In power spectral analysis it is sometimes useful to fit a power law to the spectrum to determine the spectral index

26

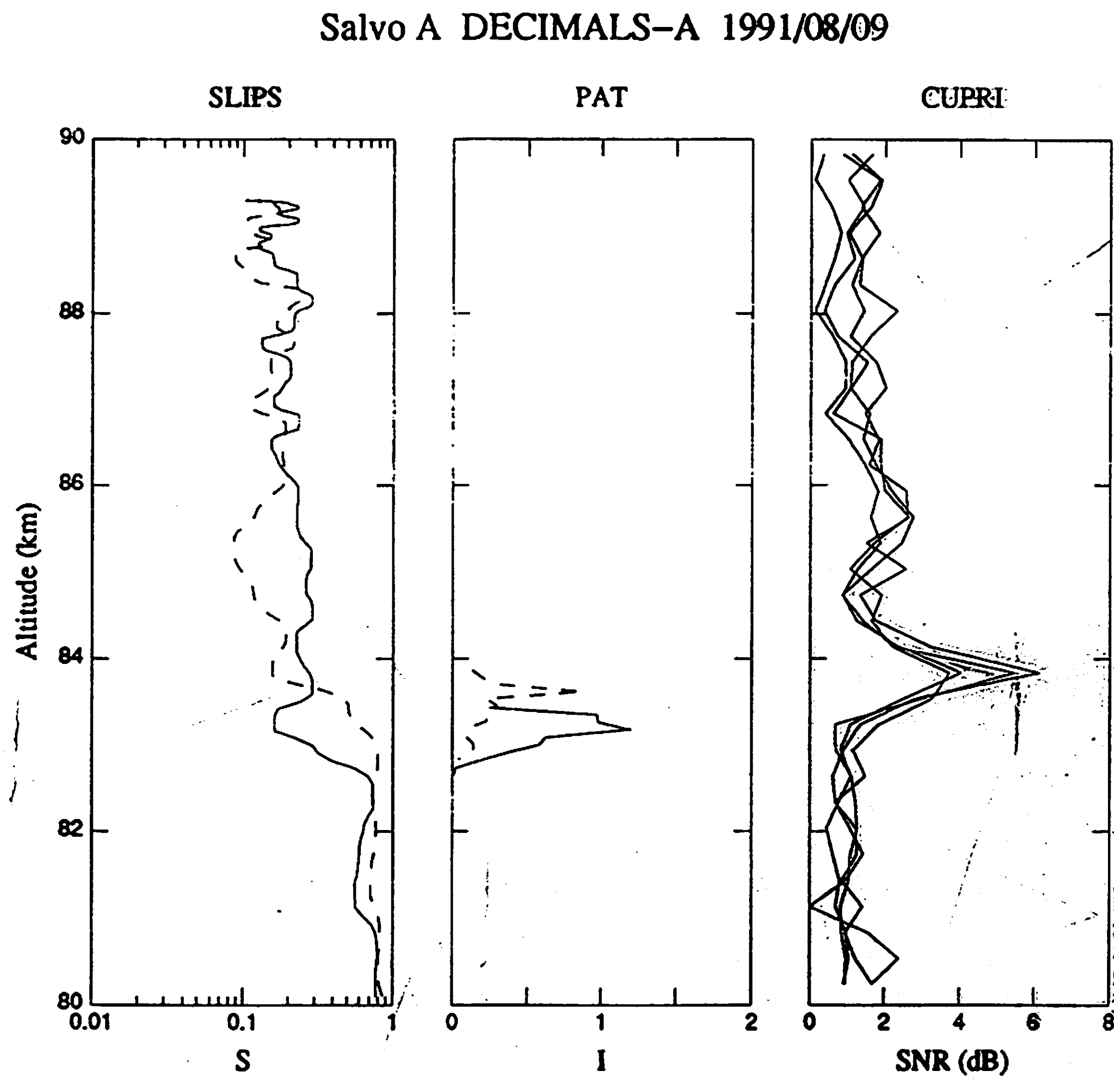

Figure 7.4: Left: Signal strength from the SLIPS (in arbitrary units). Center: Current output from the PAT (in arbitrary units). Solid lines are for the upleg and dashed lines correspond to the downleg. Right: Successive 34-s profiles of CUPRI SNR from 23:15:07 to 23:16:49 UT.

Fig. 14

27

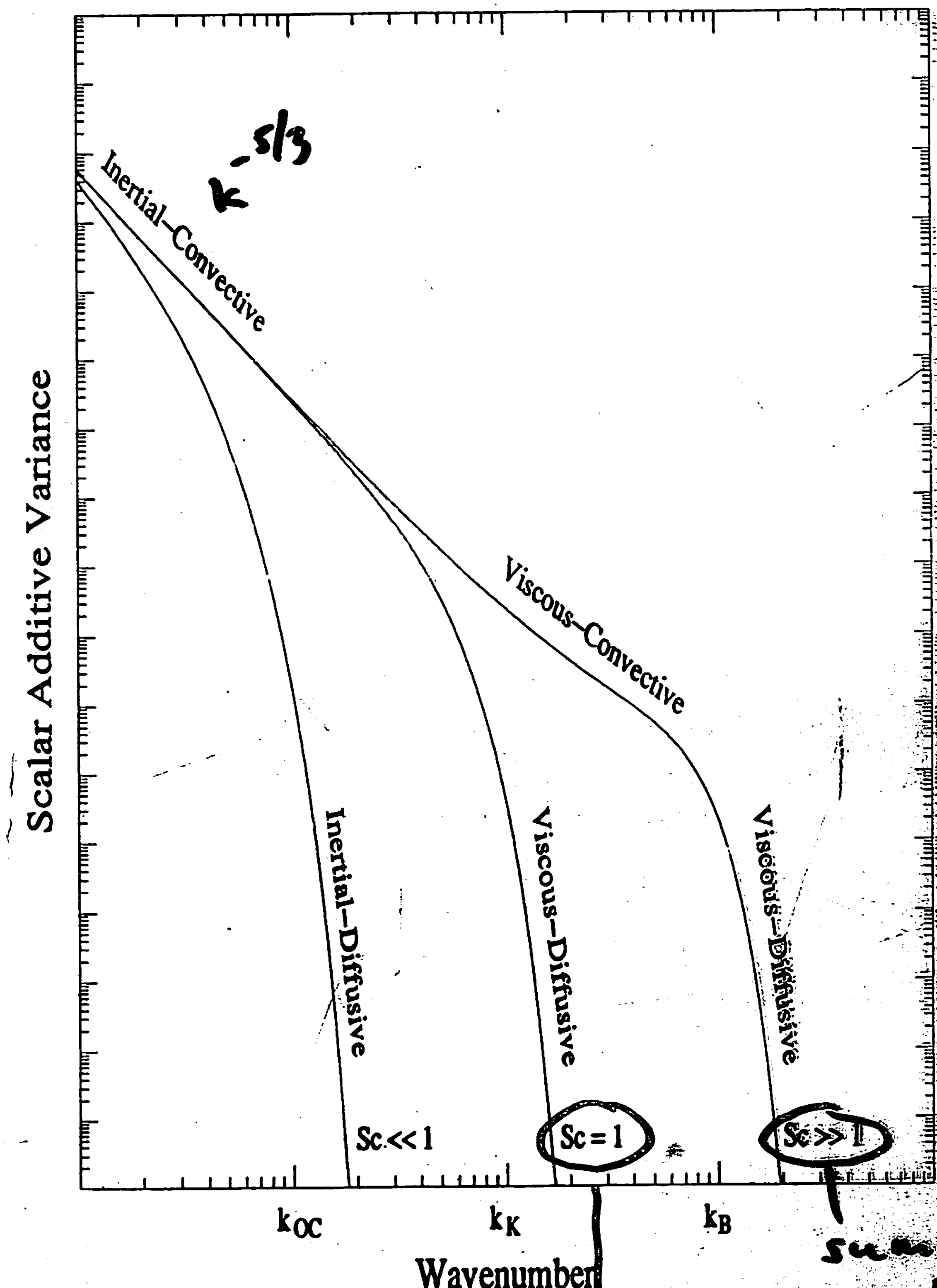

summer polar

Figure 4.1: A schematic plot showing the theoretical fluctuation energy spectra, Φ_c for a scalar additive mixed by isotropic turbulence.

non-summer non-polar

$$Sc = \frac{\nu}{D_e}$$

Fig 1

Incoherent scatter level

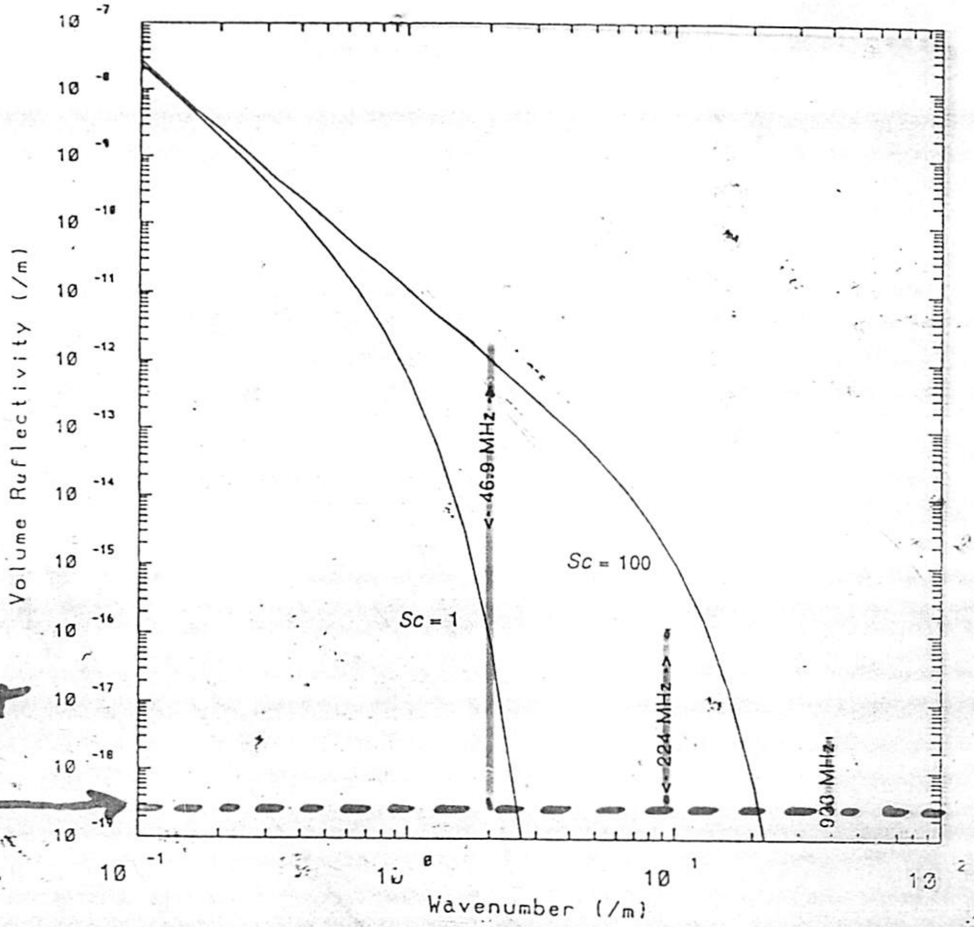

Fig. 3. Turbulent radar volume reflectivity calculated from the model of *Driscoll and Kennedy* [1985] with $N_e = 8 \times 10^9$ m^{-3}, electron scale height = 1 km, and turbulent energy dissipation rate = 1 W/kg. The data points correspond to the highest recorded echo powers at 46.9 MHz (CUPRI), 224 MHz (EISCAT VHF), and 933 MHz (EISCAT UHF).

radar reflectivity.) Also note that the curve corresponding to $Sc = 100$ matches fairly well to the 46.9-MHz and 224-MHz points but falls many orders of magnitude below that of the 933-MHz mark. (Indeed, it falls well below the reflectivity of normal incoherent scatter at this point.) On the other hand, the $Sc = 1000$ curve fits the 46.9-MHz and 933-MHz points while overshooting the 224-MHz mark. One interpretation is to ignore the 224-MHz discrepancy and take $Sc = 1000$. Another would be to take $Sc = 100$ and explain the 933-MHz PMSE as the result of enhanced incoherent scatter due to charged aerosols.

We prefer the latter argument and apply the turbulent scatter mechanism with $Sc \sim 100$ to 46.9 and 224 MHz, invoking a different mechanism for the 933-MHz PMSE. *Havnes et al.* [1990] have applied a dusty plasma theory of *Tsytovich et al.* [1989] which predicts an enhancement in the incoherent radar scattering cross section by $Z_a{}^2$. A more careful analysis by *Hagfors* [1991] shows that the scatter cross section due to charged aerosols is

$$\eta_a = \frac{Z_a{}^2 \sigma_e N_a}{\left(2 + \beta^2 - Z_a \frac{N_a}{N_e}\right)^2} \tag{23}$$

for $|Z_a| > 69 T^{\frac{1}{2}} N_a{}^{-\frac{1}{6}}$ and

$$\eta_a = \frac{Z_a{}^2 \sigma_e N_a}{\left(2 + \beta^2 - Z_a \frac{N_a}{N_e}\right)\left(2 + \beta^2 - Z_a \frac{N_a}{N_e} + Z_a{}^2 \frac{N_a}{N_e}\right)} \tag{24}$$

for $|Z_a| < 69 T^{\frac{1}{2}} N_a{}^{-\frac{1}{6}}$ where $\sigma_e = 1.0 \times 10^{-28}$ m^2 is the scattering cross section of a single electron, $\beta = k_R \lambda_D$, k_R (m^{-1}) is the radar scattering wavenumber, and

$$\lambda_D = 69 \left(\frac{T}{N_e}\right)^{\frac{1}{2}} \mathrm{m} \tag{25}$$

is the electron Debye length. Physically, (23) applies when the aerosol separation distance is greater than the aerosol Debye length such that their self-interactions can be ignored. Equation (24) is used when the aerosols must be treated as a continuum fluid.

Comparing the two expressions to the normal D region incoherent scatter cross section of *Dougherty and Farley* [1963]

$$\eta = \frac{1 + \beta^2}{2 + \beta^2} \sigma_e N_e, \tag{26}$$

we see that significant enhancement of scattered power is only possible in the first case. Thus for $N_a = 10^7$ m^{-3}, $|Z_a|$ must exceed ~ 50 for enhanced scatter. *Röttger et al.* [1990] have reported a 10-dB enhancement over the ambient incoherent scatter power (Figure 4), for the one published PMSE event at 933 MHz. According to the calibration of *Röttger et al.* [1990], $N_e = 4 \times 10^9$ m^{-3}, which yields $\beta = 0.5$. If we take $N_a = 10^7$ m^{-3}, a comparison of (23) and (26) shows we need $Z_a = 95$ or $Z_a = -120$ to yield a tenfold enhancement in radar reflectivity. This is a crude estimate of

Fig. 16

Dressed Aerosol Scatter

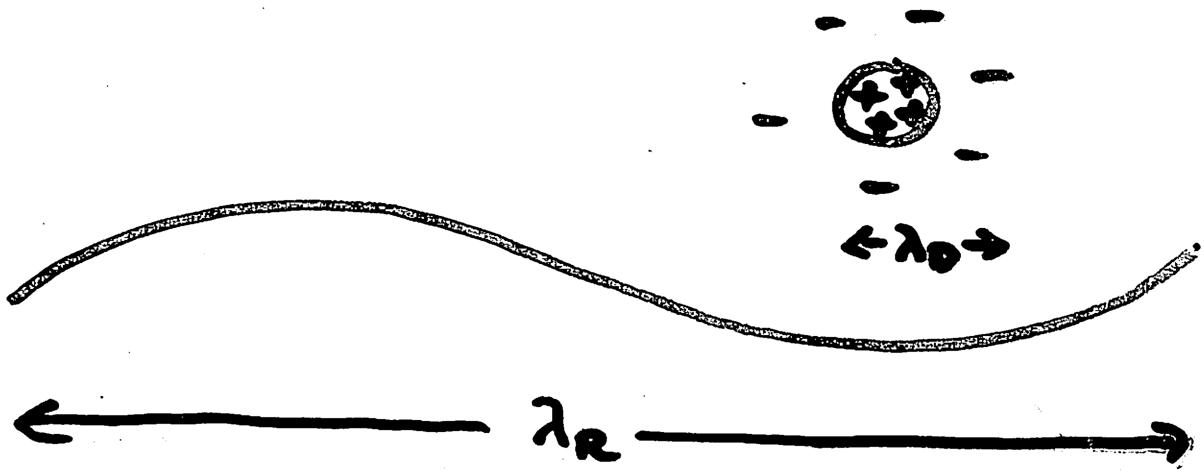

Requirements:

1. $\frac{\lambda_R}{2} \gg \lambda_D$ ✓

2. $N_a^{-1/3} \gg \lambda_D$? Sometimes.

$$\lambda_D = \left(\sum_\alpha \frac{N_\alpha Z_\alpha^2 e^2}{\epsilon_0 k T_\alpha} \right)^{-\frac{1}{2}}$$

If satisfied, enhancement over incoherent scatter by $\sim |Z_a|$.

Fig 17

But...

Existence of large charged particles also can help explain:

1. Radar-measured mean downward velocity

Ice particles form and grow. The larger aerosols fall through the cold region and sublimate at lower altitudes. The released water vapor cycles back up into the cold trap advected by the mean upward motion. Radar only observes the electron density inhomogeneities which follow only the large, falling particles. (However, particles must be fairly large ~ 0.07 μm radius, assuming spherical ice, to account for the observed downward velocity.)

[Hall et al., 1992]

Poker Flat, June
-30 cm/s

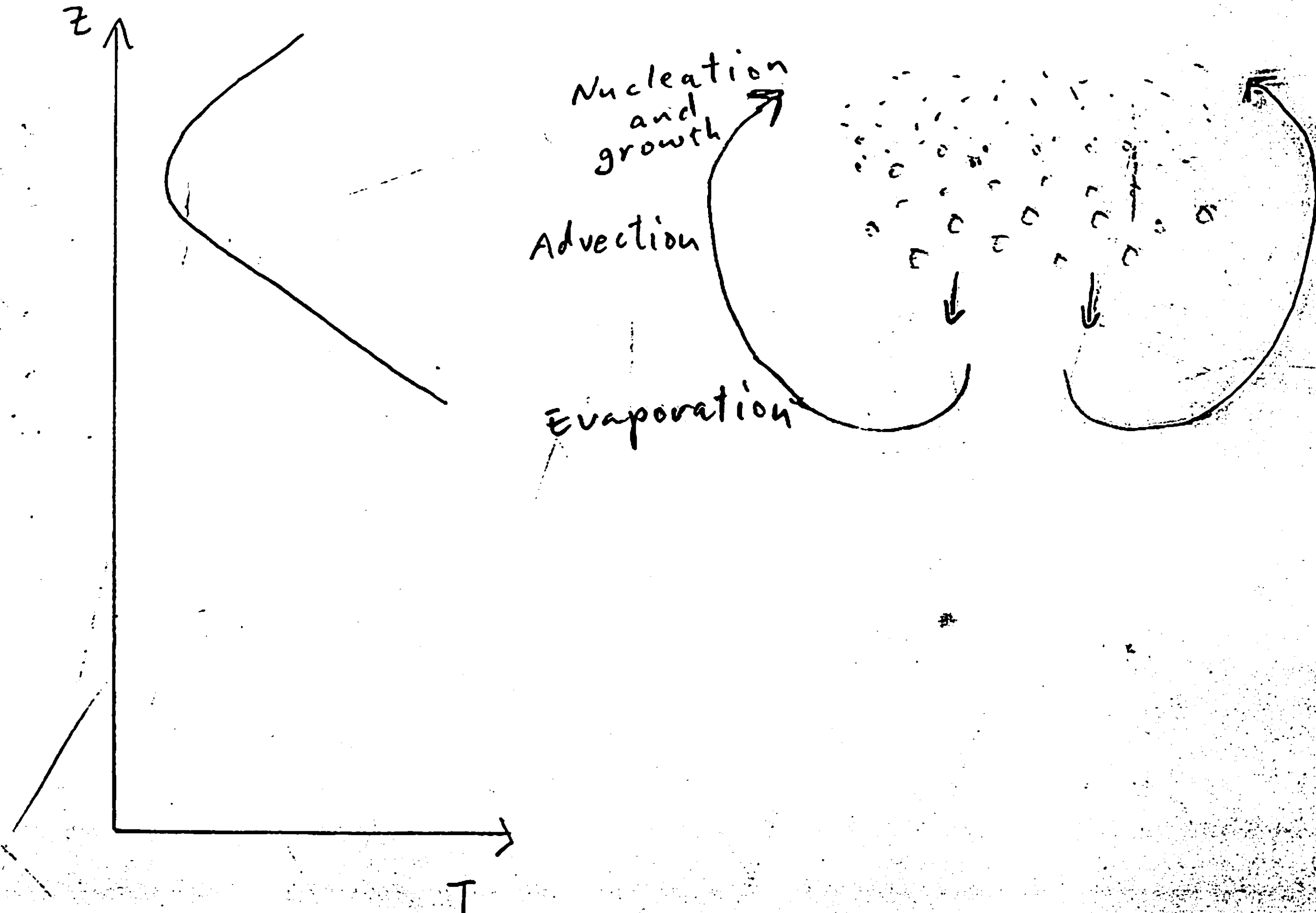

Fig. 18

Summary

- Charged aerosols can dramatically enhance radar scatter in the mesosphere.
- Their presence also helps to explain
  - electron density "bite-outs"
  - radar-observed mean downward flow

In light of non-observation in the south

PMSE → SAME

Summer
Arctic
Mesopause
Echoes

For a list of references, look for the up-coming review article:

Cho, J. Y. N, and M. C. Kelley, Polar Mesosphere Summer Radar Echoes: Theory and observations, Rev. Geophys., 1993 (in press).

Fig. 19